

## Enhancement of the red emission in $\text{CaTiO}_3:\text{Pr}^{3+}$ by addition of rare earth oxides

Xianmin Zhang<sup>a,b</sup>, Jiahua Zhang<sup>a,\*</sup>, Xia Zhang<sup>a</sup>, Li Chen<sup>a,b</sup>, Yongshi Luo<sup>a,b</sup>,  
Xiao-jun Wang<sup>a,c,\*</sup>

<sup>a</sup> Key Laboratory of Excited State Processes, Changchun Institute of Optics, Fine Mechanics and Physics, Chinese Academy of Sciences, Changchun 130033, China

<sup>b</sup> Graduate School of Chinese Academy of Sciences, Beijing 100039, China

<sup>c</sup> Department of Physics, Georgia Southern University, Statesboro, GA 30460, USA

Received 30 August 2006; in final form 29 November 2006

Available online 9 December 2006

### Abstract

Enhancement of the  $^1\text{D}_2\text{-}^3\text{H}_4$  red emission of  $\text{CaTiO}_3:\text{Pr}^{3+}$  with addition of rare earth oxides  $\text{Ln}_2\text{O}_3$  ( $\text{Ln} = \text{Lu}, \text{La}, \text{Gd}$ ) is reported.  $\text{Ca}^{2+}$  and  $\text{Ti}^{4+}$  in  $\text{CaTiO}_3$  can be substituted by  $\text{Ln}^{3+}$  ions as donors and acceptors, respectively.  $\text{Ca}^{2+}$  and  $\text{Ti}^{4+}$  vacancies, as quenching centers in the host, are effectively suppressed by the self-compensation, leading to the increase of lifetimes and then the emission efficiency of  $^1\text{D}_2$ . The red fluorescence intensity for  $\text{CaTiO}_3:\text{Pr}^{3+}$  phosphor co-doped with 5 mol%  $\text{Lu}_2\text{O}_3$  is nearly 3 times greater than that of the Lu-free samples.

© 2007 Elsevier B.V. All rights reserved.

Great attention has been paid recently on the development of advanced displays for the multimedia applications, which can replace some cathode-ray tubes (CRTs). Field emission display (FED) is one of the candidates for advanced flat-panel applications [1,2]. Therefore, the development of phosphors suitable for FED is urgently needed.

In 1994,  $\text{CaTiO}_3:\text{Pr}^{3+}$  was first reported as a promising red FED phosphor [3]. Two years later, Sung et al. optimized the preparation conditions of  $\text{CaTiO}_3:\text{Pr}^{3+}$  [4] and further stimulated the research on enhancing the red luminescence of the phosphor [5]. It was reported early that the red emission of  $\text{SrTiO}_3:\text{Pr}^{3+}$  with addition of  $\text{Al}^{3+}$  was greatly intensified compared to the Al-free samples under low-energy electron or ultraviolet light excitation [6,7]. In  $\text{SrTiO}_3:\text{Pr}^{3+}$ ,  $\text{Al}^{3+}$ ,  $\text{Pr}^{3+}$  substituted for the  $\text{Sr}^{2+}$  sites, and then the charge was balanced by the substitution of

$\text{Al}^{3+}$  for  $\text{Ti}^{4+}$  sites. The charge compensation reduced the point defects around  $\text{Pr}^{3+}$  and increased the energy transfer from  $\text{SrTiO}_3$  to  $\text{Pr}^{3+}$ . Enhancement of emission by addition of other trivalent metal ions, such as  $\text{B}^{3+}$ ,  $\text{Ga}^{3+}$  and  $\text{In}^{3+}$  in  $\text{SrTiO}_3:\text{Pr}^{3+}$  phosphor [1] and  $\text{Sc}^{3+}$ ,  $\text{Yb}^{3+}$  in  $\text{BaTiO}_3:\text{Pr}^{3+}$  phosphor [8], was also observed. The red emissions of Pr-doped  $\text{CaTiO}_3$  phosphor were stronger than that of Pr-doped  $\text{SrTiO}_3$  and  $\text{BaTiO}_3$  and even better than their enhanced emissions [6,9]. However, the emission efficiency of  $\text{CaTiO}_3:\text{Pr}^{3+}$  was low for any practical applications [5], requiring further enhancement of its red emission. Some improvements were obtained by adding metal ions such as  $\text{Na}^+$ ,  $\text{Tl}^+$  and  $\text{Ag}^+$  for charge compensation. The emission intensities were enhanced up to factors of 1.3 and 1.6 by adding  $\text{Na}^+$  or  $\text{Tl}^+$  and  $\text{Ag}^+$  to the  $\text{CaTiO}_3:\text{Pr}^{3+}$  system, respectively [5].

In this Letter, the enhancement of photoluminescence (PL) intensity is reported in  $\text{CaTiO}_3:\text{Pr}^{3+}$  phosphor with addition of rare earth oxides,  $\text{Ln}_2\text{O}_3$  ( $\text{Ln} = \text{Lu}, \text{La}, \text{Gd}$ ). It is observed that the PL intensity is nearly triple for 5 mol%  $\text{Lu}_2\text{O}_3$  added samples compared to the Lu-free samples. The emission efficiency of  $\text{CaTiO}_3:\text{Pr}^{3+}$  is

\* Corresponding authors. Address: Department of Physics, Georgia Southern University, Statesboro, GA 30460, USA (X.-j. Wang). Fax: 912 681 0471.

E-mail addresses: [zjiahua@public.cc.jl.cn](mailto:zjiahua@public.cc.jl.cn) (J. Zhang), [xwang@georgia-southern.edu](mailto:xwang@georgia-southern.edu) (X.-j. Wang).

improved by reducing the amount of defect centers. The dynamical processes of the emission are studied and the mechanisms of the fluorescence enhancement investigated.

For sample preparation, the powder mixture of  $\text{CaCO}_3$ ,  $\text{TiO}_2$ , rare earth oxides  $\text{Ln}_2\text{O}_3$  ( $\text{Ln} = \text{Lu}, \text{La}, \text{Gd}$ ), and  $\text{PrCl}_3$  solution were resolved into the de-ionized water, and then heated at  $100^\circ\text{C}$  for 3–5 h to obtain the dried powders. The powders were grounded in fume cupboard for 1 h until the pellets formed. The pellets were then sintered at  $1400^\circ\text{C}$  for 3 h under air. The doped concentration of  $\text{Pr}^{3+}$  was fixed at 0.1 mol%. The structure of the final products was characterized by powder X-ray diffractometer using a Cu target radiation source. PL, PL excitation (PLE), and diffused reflectance spectra were measured using Hitachi F-4500 fluorescence spectrophotometer. The third harmonic of a pulsed Nd–YAG laser (355 nm) together with Tektronix digital oscilloscope (model TDS 3052) was used for lifetime measurement.

Fig. 1 shows the powder X-ray diffraction (XRD) patterns of  $\text{CaTiO}_3:\text{Pr}^{3+}$  with and without the addition of 2.5 mol%  $\text{Ln}_2\text{O}_3$  ( $\text{Ln} = \text{Lu}, \text{La}, \text{Gd}$ ). The phase of  $\text{CaTiO}_3:\text{Pr}^{3+}$  is orthorhombic (JCPDS No. 82-0228). There are no extra peaks observed in the XRD patterns from the  $\text{Ln}_2\text{O}_3$  added samples, suggesting that  $\text{Ln}^{3+}$  incorporates into  $\text{CaTiO}_3$  lattice. The inset of Fig. 1 shows the shifts of the main XRD peak to the lower-angle side in the Ln-added samples compared to the Ln-free sample, which can be attributed to the lattice expansion because the ionic radii of  $\text{Ln}^{3+}$  are larger than that of  $\text{Ti}^{4+}$  in the six-coordinated state [1]. There is no significant shift of XRD peaks observed as  $\text{Ca}^{2+}$  is replaced by  $\text{Ln}^{3+}$ , since the ionic radii of  $\text{Ln}^{3+}$  are close to that of  $\text{Ca}^{2+}$  in the twelve-coordinated state [1]. Therefore, the shifts provide the evidence of  $\text{Ln}^{3+}$  substitution for the  $\text{Ti}^{4+}$  instead of  $\text{Ca}^{2+}$ . Table 1 lists the

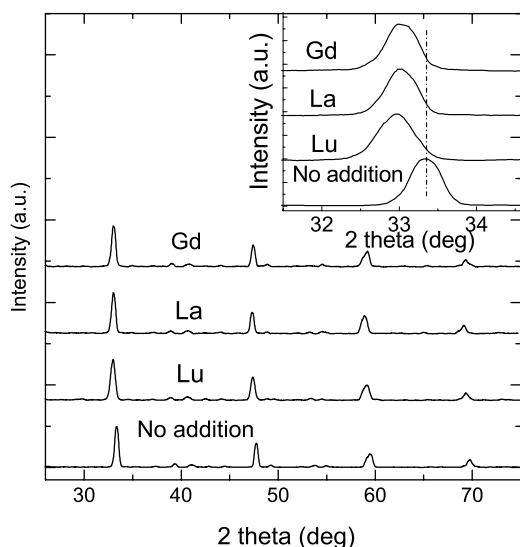


Fig. 1. Powder XRD patterns of  $\text{CaTiO}_3:\text{Pr}^{3+}$  with and without 2.5 mol%  $\text{Ln}_2\text{O}_3$  ( $\text{Ln} = \text{Lu}, \text{La}, \text{Gd}$ ) addition. Inset: expanded XRD patterns around the  $33.1^\circ$  peak of  $\text{CaTiO}_3:\text{Pr}^{3+}$ . The dashed line indicates the position of the XRD line in  $\text{CaTiO}_3:\text{Pr}^{3+}$  without  $\text{Ln}_2\text{O}_3$  addition.

Table 1

The related ion radii in the six- and twelve-coordinated states

Ion	$\text{La}^{3+}$	$\text{Gd}^{3+}$	$\text{Lu}^{3+}$	$\text{Pr}^{3+}$	$\text{Ca}^{2+}$	$\text{Ti}^{4+}$
Radius ( $\text{\AA}$ ) (VI)	1.032	1.00	0.861	0.99	–	0.605
Radius ( $\text{\AA}$ ) (XII)	1.36	$\sim 1.20$	$\sim 1.14$	$\sim 1.30$	$\sim 1.34$	–

related ion radii in the twelve and six-coordinated state [10].

To further explore the site-occupancy of  $\text{Ln}^{3+}$  ions in  $\text{CaTiO}_3:\text{Pr}^{3+}$ , the non-stoichiometrical  $\text{CaTiO}_3:\text{Pr}^{3+}$  samples with or without  $\text{Lu}_2\text{O}_3$  addition are examined Fig. 2 shows the diffused reflectance spectra of the samples with different Ca/Ti ratios. The valence-to-conduction absorption bands with edge around 330 nm are clearly presented in all the samples. In comparison with the stoichiometrical samples (Fig. 2b), there appears an extra shoulder around 380 nm in Lu free sample with Ca/Ti = 0.9 (dashed line in Fig. 2a). This shoulder can be reasonably attributed to the absorption of some defects related to  $\text{Ca}^{2+}$  vacancies, which are easily generated in the sample by the deficiency of Ca. It is found that the shoulder disappears as  $\text{Lu}_2\text{O}_3$  is added (solid line in Fig. 2a), indicating the elimination of  $\text{Ca}^{2+}$  vacancies. As a result,  $\text{Ca}^{2+}$  vacancies are considered to be occupied effectively by  $\text{Lu}^{3+}$  ions acting as donors [11]. Fig. 2c depicts that the Lu-free sample with Ti/Ca = 0.9 exhibits lower reflectance than the sample with Ca/Ti = 0.9 or Ca/Ti = 1.0. From the figure, it is speculated that  $\text{Ti}^{4+}$  vacancies have absorption in the whole visible range. When  $\text{Lu}_2\text{O}_3$  is added, the reflectance increases slightly in the spectral range, indicating that  $\text{Ti}^{4+}$  vacancies are more difficult for  $\text{Lu}^{3+}$  occupation than  $\text{Ca}^{2+}$  vacancies. Moreover, the change of body color for these phosphors is in agreement with the enhancement of

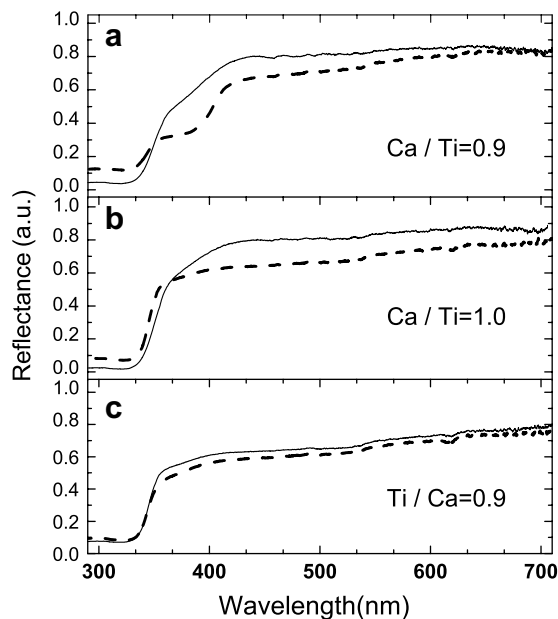


Fig. 2. Diffused reflectance spectra of  $\text{CaTiO}_3:\text{Pr}^{3+}$  with or without  $\text{Lu}_2\text{O}_3$  addition. (a) Ca/Ti = 0.9; (b) Ca/Ti = 1.0; (c) Ti/Ca = 0.9. Solid lines: 5%  $\text{Lu}_2\text{O}_3$  added samples; dashed lines: Lu-free samples.

reflectance when  $\text{Lu}_2\text{O}_3$  is added. The body colors for  $\text{Ca}/\text{Ti} = 0.9$  and  $\text{Ca}/\text{Ti} = 1.0$  samples without  $\text{Lu}_2\text{O}_3$  addition are brown and become whitish when  $\text{Lu}_2\text{O}_3$  is added; while the brown body color of the sample with  $\text{Ti}/\text{Ca} = 0.9$  has no change when adding  $\text{Lu}_2\text{O}_3$  into the host. The similar changes of body color for La or Gd-doped  $\text{CaTiO}_3:\text{Pr}^{3+}$  have also been observed.

Fig. 3 presents PL ( $\lambda_{\text{ex}} = 330$  nm) and PLE ( $\lambda_{\text{em}} = 615$  nm) spectra of  $\text{CaTiO}_3:\text{Pr}^{3+}$  with different concentrations of  $\text{Lu}_2\text{O}_3$ . The PLE spectra mainly consist of two broad bands centered at 330 nm and 370 nm, respectively. The former corresponds to the absorption of  $\text{Pr}^{3+}$  4f5d states [12] and the latter is attributed to a low-lying Pr-to-metal ( $\text{Pr}^{3+}-\text{Ti}^{4+}$ ) intervalence charge transfer state (IVCT) [13]. A group of weaker peaks are detected at 458 nm, 480 nm and 495 nm, corresponding to the  $^3\text{H}_4 \rightarrow ^3\text{P}_2$ ,  $^3\text{P}_1$ , and  $^3\text{P}_0$  transitions of  $\text{Pr}^{3+}$ , respectively [12]. The PL spectra show the intensity-calibrated red emissions peaking at 615 nm due to the  $^1\text{D}_2-^3\text{H}_4$  transition of  $\text{Pr}^{3+}$ . It is clearly exhibited that the red emissions are enhanced by the addition of  $\text{Lu}_2\text{O}_3$ . The maximum enhancement occurs in 5 mol%  $\text{Lu}_2\text{O}_3$  added sample, where the emission intensity is nearly 3 times greater than that of the Lu-free sample. In order to understand the mechanism of the fluorescence enhancement, the lifetimes of the  $^1\text{D}_2$  level of  $\text{Pr}^{3+}$  are measured for the samples with different  $\text{Lu}_2\text{O}_3$  concentrations and are plotted in Fig. 4. For comparison, the dependence of the red fluorescence intensity on  $\text{Lu}_2\text{O}_3$  concentration is also presented, showing that the lifetimes and the fluorescence intensities increase in the same scale as  $\text{Lu}_2\text{O}_3$  concentration increases. This indicates that the fluorescence enhancement is due to the increase of  $^1\text{D}_2-^3\text{H}_4$  emission efficiency. As a result, it is believed that there originally exist some defects as nonradiative recombination centers for  $^1\text{D}_2$  level of  $\text{Pr}^{3+}$ . The number of centers may be reduced by the addition of

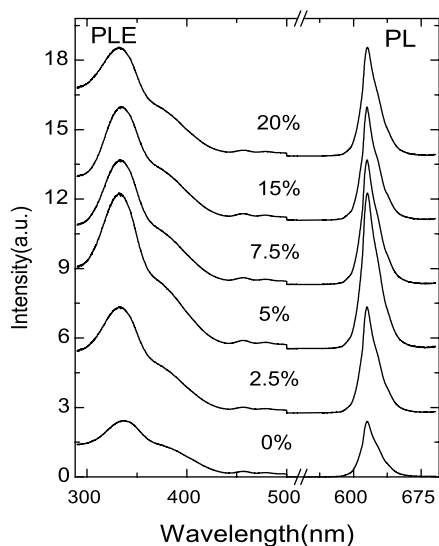


Fig. 3. PL ( $\lambda_{\text{ex}} = 330$  nm) and PLE ( $\lambda_{\text{em}} = 615$  nm) spectra of  $\text{CaTiO}_3:\text{Pr}^{3+}$  with different concentrations (0%, 2.5%, 5%, 7.5%, 15%, and 20%) of  $\text{Lu}_2\text{O}_3$ .

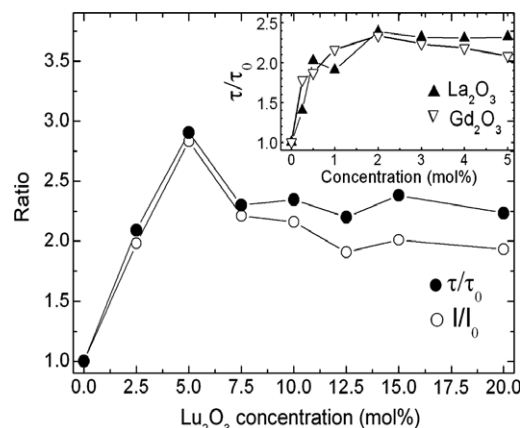


Fig. 4. The lifetimes of the  $^1\text{D}_2$  level and PL intensities of red emission ( $\lambda_{\text{ex}} = 330$  nm) in  $\text{CaTiO}_3:\text{Pr}^{3+}$  with different concentrations of  $\text{Lu}_2\text{O}_3$ . For better comparison, lifetimes ( $\tau$ ) and PL intensities ( $I$ ) are plotted as ratios to  $\tau_0$  and  $I_0$ , respectively, where  $\tau_0$  (51.87  $\mu\text{s}$ ) and  $I_0$  are the corresponding values for additive-free sample. Inset: the lifetime ratios of the  $^1\text{D}_2$  level of red emissions in  $\text{CaTiO}_3:\text{Pr}^{3+}$  with different concentrations of  $\text{La}_2\text{O}_3$  and  $\text{Gd}_2\text{O}_3$ .

$\text{Lu}_2\text{O}_3$ , leading to the increase of red fluorescence lifetimes and intensities. In  $\text{CaTiO}_3:\text{Pr}^{3+}$ ,  $\text{Pr}^{3+}$  substitutes for  $\text{Ca}^{2+}$ , creating point defects, such as  $\text{Ca}^{2+}$  vacancies or  $\text{Ti}^{4+}$ , to compensate extra positive charge of  $\text{Pr}^{3+}$ . In addition, the  $\text{Ca}^{2+}$  or  $\text{Ti}^{4+}$  vacancies can be formed during the sintering process. As shown in Fig. 2,  $\text{Lu}^{3+}$  can substitute either  $\text{Ca}^{2+}$  as donors or  $\text{Ti}^{4+}$  as acceptors [14] in  $\text{CaTiO}_3:\text{Pr}^{3+}$ ,  $\text{Lu}^{3+}$ . This self-compensation has been observed in  $\text{Sm}_2\text{O}_3$ ,  $\text{Y}_2\text{O}_3$ , and  $\text{Ho}_2\text{O}_3$  doped  $\text{BaTiO}_3$  ceramics [11,14–17]. The addition of  $\text{Ln}^{3+}$  in  $\text{CaTiO}_3:\text{Pr}^{3+}$  reduces the point defects, such as  $\text{Ca}^{2+}$  and  $\text{Ti}^{4+}$  vacancies, which act as nonradiative quenching centers for the  $^1\text{D}_2$  transition, thus enhancing the red emission efficiency. Obviously, the mechanism of fluorescence enhancement for co-doped  $\text{Lu}^{3+}$  in  $\text{CaTiO}_3:\text{Pr}^{3+}$  differs from that for co-doped  $\text{Al}^{3+}$  in  $\text{SrTiO}_3:\text{Pr}^{3+}$ , in which the increase of energy transfer efficiency between host and  $\text{Pr}^{3+}$  is considered [7]. In Fig. 4, the lifetimes and fluorescence intensities become saturated as the  $\text{Lu}_2\text{O}_3$  concentration beyond 5%, suggesting the limited solubility of  $\text{Lu}_2\text{O}_3$  in  $\text{CaTiO}_3:\text{Pr}^{3+}$ . The fluorescence enhancement by the addition of  $\text{La}_2\text{O}_3$  and  $\text{Gd}_2\text{O}_3$  is also observed, as shown in the inset of Fig. 4.

In conclusion, the enhancement of red emission in  $\text{CaTiO}_3:\text{Pr}^{3+}$  phosphor has been obtained with addition of rare earth oxides  $\text{Ln}_2\text{O}_3$  ( $\text{Ln} = \text{Lu}, \text{La}, \text{Gd}$ ).  $\text{Ln}^{3+}$  incorporates into  $\text{CaTiO}_3$  lattice by substituting either  $\text{Ca}^{2+}$  as donors or  $\text{Ti}^{4+}$  as acceptors. The substitution reduces the point defects related to  $\text{Ca}^{2+}$  and  $\text{Ti}^{4+}$  vacancies and thus enhances the red emission due to the increase of  $^1\text{D}_2-^3\text{H}_4$  transition efficiency.

#### Acknowledgements

This work is financially supported by the ‘One Hundred Talents Project’ of Chinese Academy of Sciences, the MOST of China (Contract No. 2006CB601104), the

National Natural Science Foundation of China (Grant No. 10574128) and the 863 Project.

## References

- [1] S. Okamoto, H. Yamamoto, *Appl. Phys. Lett.* 78 (2001) 655.
- [2] J.C. Park, H.K. Moon, D.K. Kim, S.C. Kim, K.S. Suh, *Appl. Phys. Lett.* 77 (2000) 2162.
- [3] A. Vecht, D.W. Smith, S.S. Chadha, C.S. Gibbons, *J. Vac. Sci. Technol. B* 12 (1994) 781.
- [4] S.H. Cho, J.S. Yoo, J.D. Lee, *J. Electrochem. Soc.* 143 (1996) L231.
- [5] P.T. Diallo, P. Boutinaud, R. Mahiou, J.C. Cousseins, *Phys. Stat. Sol. (a)* 160 (1997) 255.
- [6] S. Itoh, H. Toki, K. Tamura, F. Kataoka, *Jpn. J. Appl. Phys. Part 1* 38 (1999) 6387.
- [7] S. Okamoto, H. Yamamoto, *J. Appl. Phys.* 86 (1999) 5594.
- [8] S. Okamoto, H. Yamamoto, *J. Appl. Phys.* 91 (2002) 5492.
- [9] T. Kyomen, R. Sakamoto, N. Sakamoto, S. Kunugi, M. Itoh, *Chem. Mater.* 17 (2005) 3200.
- [10] R.D. Shannon, *Acta Cryst. A* 32 (1976) 751.
- [11] H. Kishi, N. Kohzu, Y. Mizuno, Y. Iguchi, J. Sugino, H. Ohsato, T. Okuda, *Jpn. J. Appl. Phys. Part 1* 38 (1999) 5452.
- [12] W. Jia, A. Perez-Andujar, I. Rivera, *J. Electrochem. Soc.* 150 (2003) H161.
- [13] P. Boutinaud, E. Pinel, M. Oubaha, R. Mahiou, E. Cavalli, M. Bettinelli, *Opt. Mater.* 28 (2006) 9.
- [14] K. Takada, E. Chang, D.M. Smyth, Rare earth additions to BaTiO<sub>3</sub>, in: J.B. Blum, W.R. Cannon (Eds.), *Advances in Ceramics*, vol.19, America Ceramics Society, Westerville, OH, 1987, p. P147.
- [15] S. Makishima, K. Hasegawa, S. Shionoya, *J. Phys. Chem. Solids* 23 (1962) 749.
- [16] J. Zhi, A. Chen, Y. Zhi, P.M. Vilarinho, J.L. Baptista, *J. Am. Ceram. Soc.* 82 (1999) 1345.
- [17] M.H. Lin, H.Y. Lu, *Mater. Sci. Eng. A* 335 (2002) 101.